Spectroelectrochemical Raman Study of Two End-Capped Sexithiophenes with Applications as Electroactive Molecular Materials

ARTICLE *in* THE JOURNAL OF PHYSICAL CHEMISTRY B · FEBRUARY 2002

Impact Factor: 3.3 · DOI: 10.1021/jp013028l

4 AUTHORS, INCLUDING:

Juan Casado
University of Malaga
226 PUBLICATIONS **3,637** CITATIONS
SEE PROFILE

Victor Hernandez
University of Malaga
172 PUBLICATIONS **2,965** CITATIONS
SEE PROFILE

Juan Teodomiro López Navarrete
University of Malaga
334 PUBLICATIONS **5,152** CITATIONS
SEE PROFILE

Spectroelectrochemical Raman Study of Two End-Capped Sexithiophenes with Applications as Electroactive Molecular Materials

J. Casado,[†,§] H. E. Katz,[‡] V. Hernández,[†] and J. T. López Navarrete*[,†]

Departamento de Química Física, Facultad de Ciencias, Universidad de Málaga, 29071-Málaga, Spain, AT&T Bell Laboratories, 600 Mountain Avenue, Murray Hill, New Jersey 07974, and Department of Chemistry, University of Minnesota, Minneapolis, Minnesota 55455

Received: August 7, 2001; In Final Form: November 19, 2001

In this paper, the vibrational Fourier transform Raman spectra of two sexithiophenes with the end α-positions substituted with *n*-hexyl or *n*-thiohexyl groups are studied. We investigate the effects of the different side chains on the intramolecular π-electron delocalization in neutral state and the charged defects generated upon p-doping. Density functional theory and ab initio quantum-chemical calculations are performed on various oligothiophene model compounds as an aid in the interpretation of the experimental data. The analysis of the peculiar Raman features of these π-conjugated systems has been guided by formalism of the effective conjugation coordinate theory. The Raman study of this class of materials is a powerful tool to derive information about the delocalization of π-electrons in the pristine state and the charged species upon doping.

I. Introduction

Organic low-molecular-weight and polymeric semiconductors are currently attracting increasing attention as potential active components in many electronic or optical devices including field-effect transistors (FETs).[1] In a FET device, the semiconductor layer supports a channel of holes (p-type) or electrons (n-type) between the source and drain electrodes. The density of charge carriers in the channel is modulated by the voltage applied through the gate electrode. FETs with organic semiconductors as active materials are the key switching components of organic, or plastic-based control, memory, or logic circuits.[2] The chief advantage envisioned for "plastic electronics" would be the availability of more facile fabrication methods compared to those commonly employed for traditional silicon technology, resulting in a cost advantage when the performance level and device density associated with silicon are not essential.

The most important criteria for a FET semiconductor are high charge carrier mobility, high current modulation (on/off current ratio), stability, and processability. The processing advantages of organic materials can be gained most fully through the use of solution or liquid phase deposited semiconductors to fabricate devices using low-cost techniques such as casting, spin-coating, and printing.[3]

In this regard, the research efforts of one of us (Katz's group) in FETs have been focused on identifying organic molecular materials with high performance, good solubility, and potential liquid phase processability, as well as long-term stability. From the earliest development of a thin film transistor based on sexithiophene,[4] many other attempts have been reported in the literature.[5] In this sense, thiophene oligomers with solubilizing end substituents are among the more promising FET materials. Moreover, unlike the thiophene polymers, impurities in these oligothiophenes can be relatively easily removed by sublimation under reduced pressure. The monodisperse conjugation length of these molecules allows them to organize into almost defect-free layered structures. Thin film FETs with high mobility can be routinely obtained by evaporation or by casting dilute solutions of these oligothiophenes. For instance, the highest mobilities (ca. 0.03 $cm^2/V \cdot s$) were achieved with α,α′-dihexyl end-capped sexithiophene, which was found to be slightly higher than that of the prototypical organic semiconductor, i.e., the unsubstituted sexithiophene.[5]

Oligothiophenes have also been used as active materials in other electrooptical devices such as light emitting diodes (LEDs).[6−8] The electronic and optical responses of the organic films based on oligothiophenes depend on many variables (e.g., molecular order and packing, evaporation rate, thin film thickness).[9,10] However, two of the most relevant factors that determine the efficiency of the FET and LED devices are the degree of intramolecular π-electron delocalization and the type of charge carriers involved in the microscopic mechanisms that take place upon application of a strong electric or magnetic field or upon doping.[11,12]

In this scenario, experimental studies of the dependence of the optical and electronic properties of the oligothiophenes on their chemical structures and substitution patterns are important to improve the structure−property relationship of these materials and their use in technological applications.

Raman spectra of polyconjugated compounds show unusual features directy related to the degree of π-electron delocalization in neutral state and the charged carriers created upon doping or photoexcitation.[13] It is hard to get detailed structural information on a doped material in terms of bond lengths and angles by means of many usual experimental techniques. However, the combination of quantum-chemical calculations with vibrational spectroscopic data provide a very valuable source of structural information. In fact, this strategy of study is one of the most powerful tools to prove, on a molecular scale, the electronic and structural modifications after chemical or electrochemical doping.[14−16]

In papers central to the understanding of the peculiar vibrational spectra of neutral, doped, and photoexcited conju-

* To whom correspondence should be addressed.
[†] Universidad de Málaga.
[‡] AT&T Bell Laboratories.
[§] University of Minnesota.

10.1021/jp013028l CCC: $22.00
Published on Web 02/16/2002

gated systems, Zerbi et al. developed the effective conjugation coordinate theory (ECC).[17] In aromatic and heteroaromatic conjugated systems, the ECC mode has the analytic form of a linear combination of ring C═C/C−C stretchings which points in the direction from the benzenoid structure (usually that of the ground state) to the quinonoid structure (that corresponding to the electronically excited state or the oxidized species). On going from neutral to doped forms, the molecular backbone of the oligomer changes from an aromatic to a quinonoid structure. Along this structural modification of the π-conjugated molecular system the double C═C bonds are weakened, while the single C−C bonds are strengthened. Therefore, upon chemical or electrochemical doping, the frequency of the Raman bands associated with molecular vibrations with a large content of ν(C═C) motions (i.e., those mainly involving the ECC mode) shift downward. Thus, a sizable downshift for the Raman bands associated with the dynamics of the ECC mode must be expected on going from neutral to doped species.

Current quantum-chemical methods are in the position to give reliable information about the molecular structure and vibrational properties of the different classes of π-conjugated systems. The ability of calculating molecular force fields and geometries is likely one of the most important developments in computational chemistry over the past decade. Most current calculations are performed within the ab initio restricted Hartree−Fock (RHF) scheme. At this level of theory, the calculated harmonic force constants and vibrational frequencies are usually higher than the corresponding experimental values, due to a combination of electron correlation effects and basis set deficiencies. Nonetheless, as the errors of these calculations are largely systematic, they can be corrected after inclusion of appropiate scaling factors.[18] On the other hand, density functional theory (DFT) is an alternative to the HF method for adding electron correlation effects. DFT studies have proved very useful in the case of the study of charged molecules.[19,20]

In this article, we analyze the vibrational Raman spectra of two end-capped sexithiophenes in relation to the effects of the α,α′-disubstitution (*n*-thiohexyl vs *n*-hexyl groups) on the π-electron conjugation in neutral state. An exhaustive electrochemical oxidation of both oligothiophenes was carried out. The Raman spectra of the oxidized materials are interpreted on the basis of the ECC theory to elucidate the types of charged defects generated upon p-doping and the role of the side chains in their stabilization. As a support to the analysis of the experimental spectra, we also report on the main results of a quantum-chemical study performed on two quaterthiophene model systems α,α′-disubstituted with methyl or *n*-thiopropyl groups (referred to as DMQtT and DPTQtT henceforth, respectively).

II. Experimental and Computational Details

The hexamers were synthesized following the experimental procedure described elsewhere.[21] Chemical structures of the α,α′-dithiohexyl and α,α′-dihexyl end-capped sexithiophenes (here after named as DHTSxT and DHSxT, respectively) are shown in Figure 1, together with that of the α,α′-dimethyl end-capped sexithiophene (DMSxT). The last compound has been previously studied by our group, and it will be taken as a model sexithiophene bearing a short α-alkyl side chain.[22]

FT-Raman measurements were performed using a Bruker FRA 106/S apparatus and a Nd:YAG laser source (λ_{exc} =1064 nm), with an operating power of 100 mW. To improve the signal-to-noise ratio, 500 scans were averaged. All FT-Raman spectra were acquired in a typical backscattering configuration.

Cyclic voltammetries and Raman spectroelectrochemical experiments were performed on thin solid films at room temperature in contact with a 0.1 M tetrabutylamonium tetrafluoroborate ($TBABF_4$)−acetonitrile solution. The films of the sexithiophenes were obtained by solvent evaporation from a 1,2-dichloromethane dispersion. Two platinum electrodes were used as working and auxiliary electrodes. All electrochemical measurements were carried out using an SCE reference electrode with a scan rate of 100 mV/s. The experimental procedure was as follows: the oligomer-coated platinum electrode was immersed into the 0.1 M $TBABF_4/CH_3CN$ solution, and a fixed anodic potential was applied for 60 s just before each Raman measurement. The voltammetric waves previously obtained for both sexithiophenes were used to choose the anodic potential values for the progressive oxidation of the films. After every electrochemical oxidation, the FT-Raman spectrum was directly recorded on the coated Pt electrode. In all experiments, Voltalab40 electrochemical equipment from Radiometer was employed.

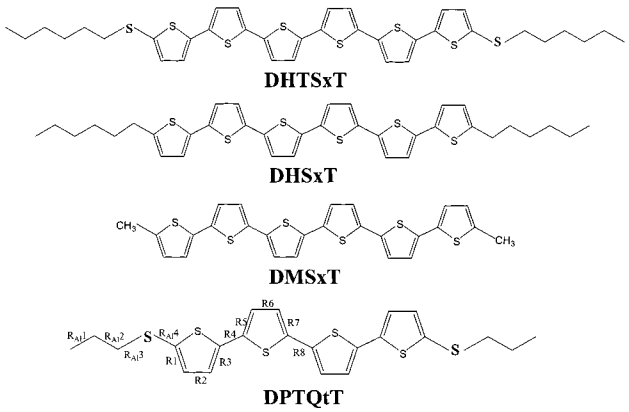

Figure 1. Chemical structures of DMSxT, DHSxT, DHTSxT, and DPTQtT.

Restricted Hartree−Fock ab initio calculations for the neutral systems and DFT calculations (using the B3LYP functional) for the doped species were carried out with the Gaussian 98 program running on a SGI Origin 2000 supercomputer.[23] A 6-31G** basis set was used.[24] This basis set includes a set of six second-order (d-type) Gaussian primitive functions for the description of each heavy atom and a single set of Gaussian p-polarization functions for hydrogens. Geometry optimizations were performed on isolated entities. Due to the large cost of the force field calculations, only the all-anti coplanar conformations were evaluated analytically within the same theoretical scheme used for the geometry optimizations. The theoretical frequency values were scaled down uniformly by a factor of 0.9 for the neutral compound and a factor of 0.96 for the doped species, as recommended by Scott and Radom.[25] This approach is very attractive in large-scale studies because it avoids the complex procedure of defining internal vibrational coordinates. All quoted vibrational frequencies reported throughout the paper are, thus, scaled values.

III. General Considerations

III.a. Molecular Structures and Selection Rules. No experimental X-ray or electron diffraction data are available for DHSxT and DHTSxT. Supposedly, as shown by the X-ray structure of some related compounds (such as the unsubstituted α-oligothiophenes,[26] α,α′-dimethyl end-capped quaterthiophene,[27] and α,α′-dihexylquaterthiophene[4]), it can be assumed that (a) the thienyl sulfur atoms are located in an all-anti configuration with respect to the long molecular axis and (b) the whole molecule retains a coplanar conformation of the aromatic units.

With such a structure the two sexithiophenes belong to the C_{2h} symmetry point group. Nevertheless, the rings at both ends of the oligothiophene chain likely display a slight bent relative to the inner ring least-squares plane. Thus, the strict C_{2h} symmetry could be partially broken. However, in what follows, it will be assumed that both molecules present internal symmetry in the solid state. For DHTSxT, there exist 246 vibrational normal modes. Of them, 123 are IR-active and 123 are Raman-active as deduced from the optical selection rules for C_{2h} molecular symmetry.

III.b. Vibrational Considerations. Although the optical selection rules predict a very large population of bands in the Raman spectra, the experimental patterns are fairly simple. This seeming discrepancy between theoretical predictions and experimental observations needs to be accounted for:

(i) Since the two side chains at the end α,α′-positions are relatively far apart, no mechanical coupling is expected to occur between their characteristic vibrations. Therefore, in-phase and out-of-phase motions of the side chains should be degenerate and would not show any splitting in the spectra.

(ii) It is reasonable to think that a hexameric chain is not too large to observe progressions of bands (set of close bands with frequency differences of about 4−5 cm^{-1}) associated with the same type of oscillators with different phase angles.

(iii) In the case of neutral π-conjugated compounds with symmetric chemical structures, the molecular symmetry does not chage from the ground to the lower lying excited electronic states, and thus only totally symmetric normal modes should be selectively enhanced by Raman resonance.[28] In the case of the doped compounds, resonance conditions between the exciting laser line and some electronic absorptions of the oxidized species are generally fulfilled, and therefore only a few Raman modes gain appreciable intensity relative to the remaining Raman-active vibrations.[29]

(iv) The π-conjugated organic materials (oligomers and polymers) show for a few Raman lines an overwhelming enhancement with respect to the other Raman-active molecular vibrations and sizable frequency and intensity dispersions with chain length.[14] These phenomena have been fully accounted for by the theoretical formalism of the above-mentioned ECC theory on the basis of the existence of a very effective electron−phonon coupling between the π-electron system and the molecular vibrations.[14]

These facts could account for the rather simple appearance of the actual Raman spectra of the π-conjugated materials as compared with the large population of active molecular vibrations predicted by group theory.

IV. Raman Spectra of the Neutral Material

Attempts to obtain Raman spectra with exciting radiations in the visible region were unsuccessful due to the high fluorescence showed by the samples. To obtain the vibrational information, the use of laser exciting wavelengths in the near-IR region was necessary. In this work, a Nd:YAG laser with an excitation wavelength of 1064 nm was employed.

Figures 2 and 3 show the FT-Raman spectra of DHSxT and DHTSxT in neutral state together with those of unsubstituted sexithiophene (SxT) and DMSxT as reference compounds.[30,31] Figure 4 shows the theoretical RHF/6-31G** Raman spectra of neutral DPTQtT and DMQtT, while Figure 5 shows the RHF/6-31G** vibrational displacements (eigenvectors) associated with the main totally symmetric Raman-active vibrations of neutral DPTQtT. Table 1 summarizes a correlative analysis of

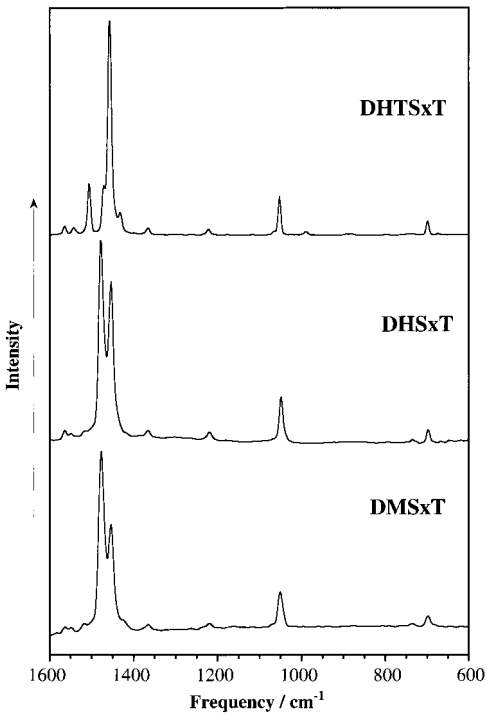

Figure 2. FT-Raman spectra, over probe energies of 1600−600 cm^{-1}, of DMSxT, DHSxT, and DHTSxT in neutral state (λ_{exc} = 1064 nm).

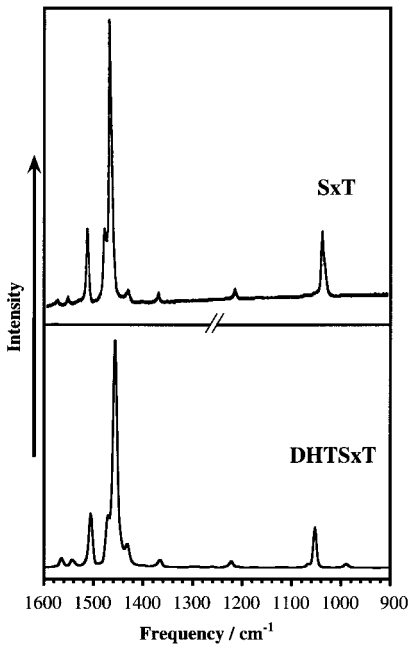

Figure 3. Comparison between FT-Raman spectra of DHTSxT and SxT in neutral state (λ_{exc} =1064 nm).

the Raman frequencies measured in the solid-state spectra of neutral DHSxT and DHTSxT together with their tentative full assignment.

In a first look at Figures 2 and 3, we notice that the Raman spectra of DHSxT and DMSxT are almost identical, the only difference being that the band at 1453 cm^{-1} in DHSxT is sligthly more intense than that at 1454 cm^{-1} in DMSxT. On the other hand, the Raman spectra of SxT and DHTSxT are also rather similar to each other.

The Raman spectra of the oligothiophenes are characterized by the appearance of four strong lines usually termed lines A, B, C, and D.[31−36] Line A is generally weak and undergoes a

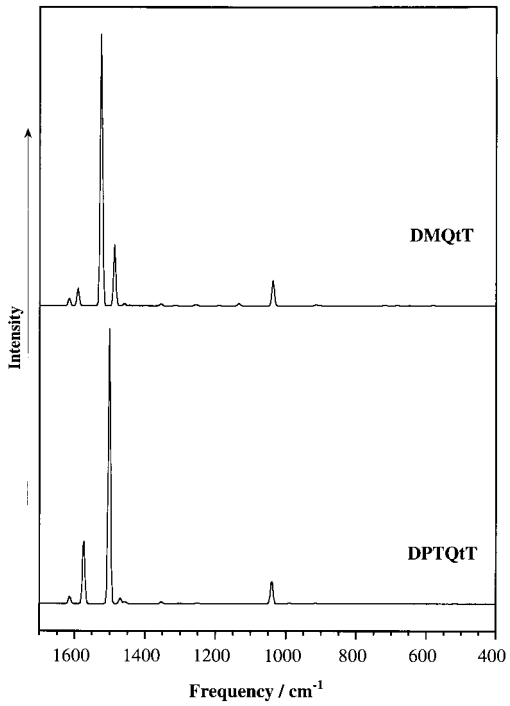

Figure 4. Theoretical RHF/6-31G** Raman spectra of DMQtT and DPTQtT.

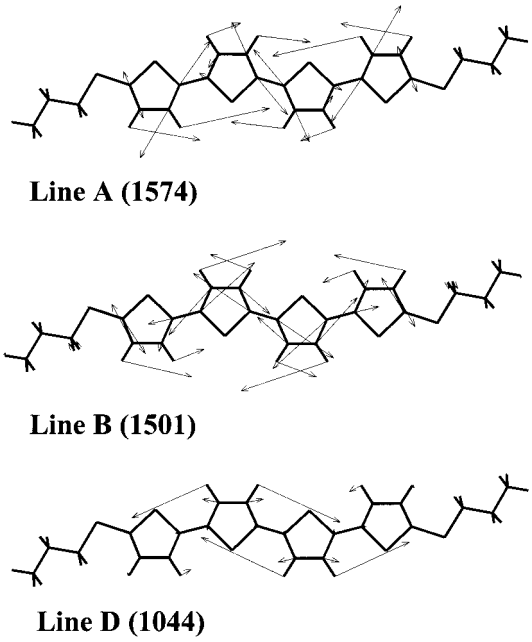

Figure 5. Schematic atomic displacements for the characteristic totally symmetric Raman-active normal modes usually labeled as lines A, B, C, and D of neutral DPTQtT, calculated at the RHF/6-31G** level.

sizable downshift with increasing chain length. In the hexamers studied in this work, line A must be assigned to the scatterings at 1514 and 1507 cm^{-1} in DHSxT and DHTSxT, respectively. This Raman vibration should be correlated to the line calculated at 1574 cm^{-1} in DPTQtT and due to an in-plane antisymmetric ν(C═C) stretching mainly located on the outermost thiophene ring of the chain (see Figure 5).[35,36]

Line B is always the strongest one of the Raman spectrum. While it largely downshifts with increasing chain length in the oligopyrroles and the oligofurans, for the oligothiophenes its peak position is almost independent of the molecular size and quickly meets saturation.[35] Furthermore, for all types of

TABLE 1: Correlation between the Vibrational Raman Frequencies of the Neutral DHSxT and DHTSxT and the Tentative Assignment of the Main Raman Bands

DHSxT	DHTSxT	assignment
1564	1564	
1549	1542	
1514		
	1507	line A
1478		*line B*
	1470	
	1456	*line B*
1453		line C
	1431	
1366	1365	
1219	1221	
1049	1052	line D

π-conjugated materials, the relative intensity of line B continuously increases as the length of the oligomer grows longer (at least from the dimer to the hexamer).[36] The position of line B is also dependent on the substitution pattern: it generally appears at higher frequencies in the class of the α and/or β end-capped oligothiophenes than in the unsubstituted pattern oligomers.

In the case of the two sexithiophenes studied in this work, line B has been assigned to the Raman bands at 1478 cm^{-1} in DHSxT and 1458 cm^{-1} in DHTSxT. Line B is calculated at 1501 cm^{-1} for DPTQtT, and it can be described as a fully in-phase symmetric ν(C−C) mode spreading over the whole oligomeric chain. The motions of the CC bonds are necessarily coupled with the in-plane bending of the aromatic C−H bonds, in which the H atoms recoil with a large vibrational displacement which opposes that of the C_β atoms. This normal mode corresponds to the collective *R* coordinate of the ECC theory. Line B is predicted to appear at 1525 cm^{-1} in the RHF/6-31G** Raman spectrum of DMQtT (see Figure 4). Thus, the theoretical calculations envisage a dispersion toward lower frequencies by 24 cm^{-1} on going from DMQtT to DPTQtT, in excellent agreement with the experimental downshift by 20 cm^{-1} on going from DHSxT to DHTSxT.

As aforementioned, the Raman spectral patterns of DHTSxT and SxT are nearly the same, while those of DMSxT and DHSxT are rather similar to each other. The eigenvector associated with line B in DPTQtT shows that during this molecular vibration only the conjugated C═C/C−C bonds move with large displacements with respect to their equilibrium positions, while the aliphatic C−C and C−S bonds remain almost motionless. It could be argued that since the S atom is heavier than C, if a *stone* is placed between two springs they will turn out to be mechanically decoupled. However, the molecular dynamics of one-dimensional oligomeric chains with *free ends* is expected to be different from those with *fixed ends*, especially in the case of very short chains (like a hexamer). We believe that this experimental finding is due to the decoupling of the electronic interaction between the alkyl side chain and the π-conjugated backbone when a sulfur atom is intercalated between them, thus meaning that S can act as an effective electronic spacer.

Line C is generally recorded at the lower energy side of line B for the class of α and/or β end-capped oligothiophenes. It becomes stronger and experiences a slight upshift in frequency as the number of thiophene units in the chain increases. Line C also seems to be stronger as the alkyl side chain grows. We believe that the selective Raman enhancement of this line with respect to the other Raman-active vibrations is a consequence of the electronic interaction between the π-conjugated spine of the molecule and the alkyl end groups. This characteristic Raman

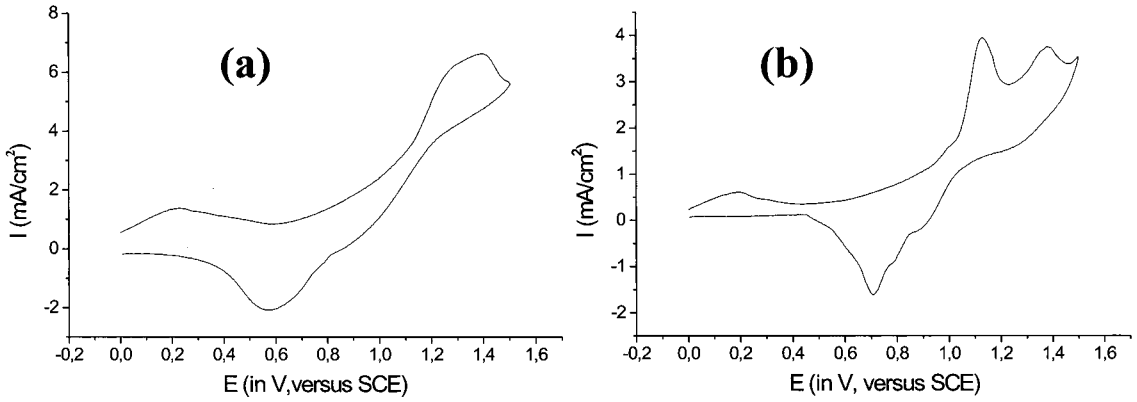

Figure 6. Cyclic voltammograms of (a) DHSxT and (b) DHTSxT as thin films in contact with a 0.1 M $TBABF_4/CH_3CN$ solution, over the 0−1.5 V potential range (potential values vs SCE). Scan rate: 100 mV/s.

vibration is assigned to the scatterings at 1453 and 1458 cm^{-1} in DHSxT and DMQtT, respectively. The normal mode associated to line C could be described as a collective symmetric ν(C═C) vibration spreading over the whole oligothiophene chain in which the motions of the sucessive thiophene rings take place out of phase. As in the case of the unsubstituted oligothiophenes (where line C is absent), no Raman scattering related to line C is observed in DHTSxT, giving further support to the conclusion that the attachment of S atoms at the end α-positions of the π-conjugated backbone switches off the interaction with the end groups.

Finally, line D appears for all classes of oligothiophenes as a sharp band of medium-strong intensity around 1050−1080 cm^{-1}, its peak position being little dependent on the substitution pattern and chain length of the oligomer. This line is measured for DHSxT at 1050 cm^{-1} and for DHTSxT at 1052 cm^{-1}. In view of the calculated eigenvectors, line D has to be assigned to the RHF/6-31G** theoretical band calculated at 1044 cm^{-1} that should be described like a fully in-phase symmetric in-plane bending mode of the C−H bonds attached to the different β-positions of the inner thiophene rings. Its strong local mode character justifies their almost constant frequency of appearance.

V. Spectroelectrochemical Study of the Doped Materials

V.a. Electrochemical Study. Figure 6 shows the cyclic voltammetry waves of DHSxT and DHTSxT as solid thin films in contact with a 0.1 M $TBABF_4/CH_3CN$ solution. Cyclic voltammograms (CV) are reproducible over the 0−1.5 V potential range, thus indicating that the electrochemical processes which take place in the doping are reversible. The CV of DHSxT shows a maximum on oxidation at 1.39 V together with an unresolved peak at 1.28 V, while on the reduction branch a minimum at 0.58 V and a shoulder at 0.87 V are noticed. The potentials of the oxidation peaks of DHSxT are shifted to more anodic values as compared with those of DMSxT, likely due to the higher compaction of the solid film and the use of a different electrochemical medium.[37]

The CV of DHTSxT shows two well-resolved maxima on oxidation at 1.13 and 1.38 V, while on the reduction branch a minimum at 0.711 V and two shoulders at 0.78 and 0.88 V are observed. The two oxidation peaks in DHTSxT are shifted to lower anodic potential values with respect to those of DHSxT. This downshift could be the result of the participation of the α-sulfur atoms in the stabilization of the oxidized species generated upon doping. When an oligothiophene is oxidized, positive charges are injected into the π-conjugated system; the sulfur atoms attached at the end α-positions of the oligomer likely act as electron donors, thus stabilizing the electronic defects. The voltammograms display certain asymmetry between the oxidation and the reduction branches due to the hysteresis processes in the solid state.

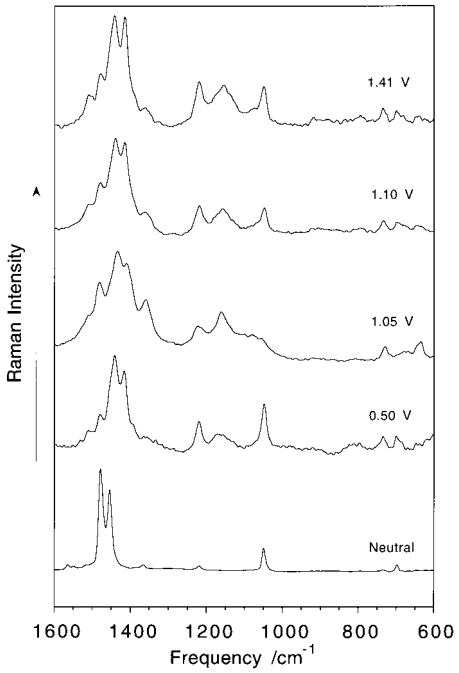

Figure 7. Evolution of the Raman spectrum of DHSxT during the electrochemical oxidation of the compound from the neutral state to 1.5 V (potential values vs SCE).

V.b. Spectroelectrochemical Raman Study. Figures 7 and 8 show the Raman spectra of DHSxT and DHTSxT at selected anodic potentials. On the other hand, Tables 2 and 3 summarize the vibrational Raman frequencies of neutral DHSxT and DHTSxT and of those of electrochemically doped DHSxT and DHTSxT at different anodic potentials, respectively.

For DHSxT oxidized at 1.05 V, the strongest band is recorded at 1442 cm^{-1}, together with a second strong component at 1417 cm^{-1}. At higher oxidation levels (i.e., 1.41 V) the Raman spectra pattern displays only very subtle changes and the line at 1415 cm^{-1} gains intensity with respect to the Raman band at 1442 cm^{-1}. On the other hand, the scatterings at 1480 and 1360 cm^{-1} gain intensity in the doped species.

For DHTSxT oxidized at 1.01 and 1.13 V, three new Raman lines as compared with the spectrum of the neutral form are recorded at 1427, 1397, and 1355 cm^{-1} in the high energy region of the spectrum above 1300 cm^{-1}, the former being the strongest one of the spectrum. Nonetheless, some Raman lines of the

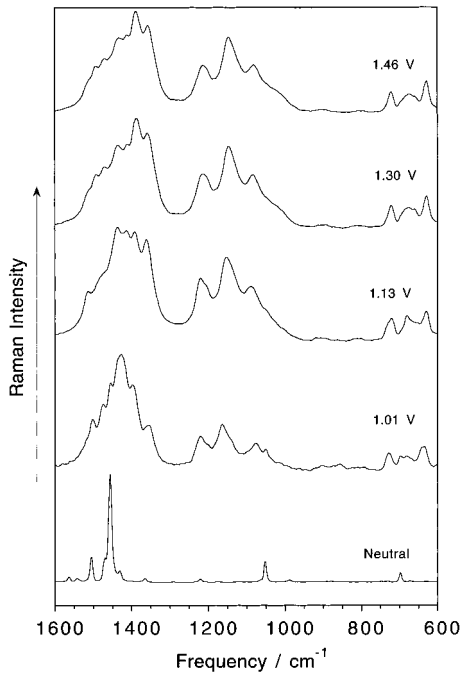

Figure 8. Evolution of the Raman spectrum of DHTSxT during the electrochemical oxidation of the compound from the neutral state to 1.46 V (potential values vs SCE).

TABLE 2: Correlation between the Vibrational Raman Frequencies of Neutral DHSxT (DHSxT-N) and Those of Electrochemically Doped DHSxT at Different Anodic Potentials (*E* in volts)

DHSxT-N	$E = 1.05$	$E = 1.10$	$E = 1.41$
1564			
1549			
1514	1510	1510	1510
1478[a]	1479	1481	1481
1453			
	1442[a]	1435	1438
	1417	1410	*1415*[a]
1366	1363	1360	1361
			1309
			1276
1219	1220	1223	1218
	1158	1162	1162
		1100	1090
		1080	1077
1049	1048	1056	1048

[a] In italics, the frequency of the most intense band of each Raman spectrum.

neutral species are still observed (i.e., 1474 and 1455 cm^{-1}), as a consequence of the hysteresis processes associated with the electrochemical oxidation of an oligomeric film (and the hard difussion of electrons and counterions through a solid-state matrix). Between 1.30 and 1.46 V, the Raman spectral pattern further changes, and now the lines centered at around 1390 and 1360 cm^{-1} become the strongest ones among the different C═C stretching vibrations of the system (particularly that at the higher frequency). No Raman lines of the neutral species are observed at high oxidation potentials.

Below 1300 cm^{-1}, the main spectral difference between the doped and neutral materials is the appearance of three medium-strong Raman lines around 1220, 1150, and 1080 cm^{-1}. These "doping Raman lines" are clearly seen in the spectra of DHSxT and DHTSxT at the various anodic potentials. Of them, those at 1220 and 1080 cm^{-1} seemingly already exist in the neutral material, but they gain appreciable intensity upon doping. On the other hand, that at 1150 cm^{-1} arises from the oxidized species and it is completely absent in the Raman spectrum of the neutral form.

TABLE 3: Correlation between the Vibrational Raman Frequencies of Neutral DHTSxT (DHTSxT-N) and Those of Electrochemically Doped DHTSxT at Different Anodic Potentials (*E* in volts)

DHTSxT-N	$E = 1.01$	$E = 1.13$	$E = 1.30$	$E = 1.46$
1564				
1542				
1507	1502	1513		1513
			1493	1493
1470	1474		1470	1471
1456[a]	1455			
1431	*1427*[a]	*1431*[a]	1432	1436
		1413	1412	1413
	1397	1392	*1388*[a]	*1387*[a]
1365				
	1355	1362	1357	1359
1221	1220	1221	1214	1214
	1164	1153	1153	1147
	1077	1089	1081	1083
1052				

[a] In italics, the frequency of the most intense band of each Raman spectrum.

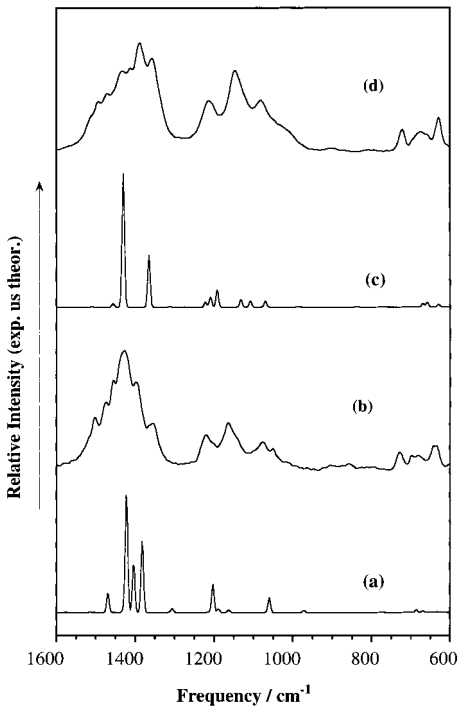

Figure 9. Comparison of the (a) theoretical UB3LYP/6-31G** Raman spectrum of the radical cation DPTQtT, (b) experimental Raman spectrum of doped DHTSxT at low oxidation potential, (c) theoretical B3LYP/6-31G** Raman spectrum of the dication of DPTQtT, and (d) experimental Raman spectrum of doped DHTSxT at high oxidation potential.

The Raman spectra of the doped species obtained along the reduction branch for DHSxT and DHTSxT are quite similar to those previously recorded during the oxidation branch. Therefore, the same types of charged defects must be involved in the initial oxidation and subsequent reduction of both materials.

V.c. Theoretical Raman Spectra of the Doped Species. Figure 9 shows the DFT Raman spectra of DPTQtT as radical cation (UB3LYP/6-31G**) and dication (B3LYP/6-31G**) together with the actual Raman spectra of DHTSxT at low and high oxidation potential values.

TABLE 4: Comparison of DFT Calculated Bond Lengths (in Å) for DPTQtT in Neutral State (B3LYP/6-31G), as Radical Cation (UB3LYP/6-31G**) and as Dication (B3LYP76-31G**)**

bond[a]	DPTQtT	$DPTQtT^{\bullet+}$	$DPTQtT^{2+}$	increment[b]
$R_{Al}1$	1.539	1.539	1.539	0
$R_{Al}2$	1.532	1.532	1.532	0
$R_{Al}3$	1.837	1.844	1.853	+0.016
$R_{Al}4$	1.765	1.740	1.712	−0.053
R1	1.375	1.390	1.417	+0.042
R2	1.422	1.401	1.379	−0.043
R3	1.377	1.395	1.417	+0.040
R4	1.443	1.418	1.394	−0.049
R5	1.381	1.405	1.430	+0.049
R6	1.415	1.389	1.368	−0.047
R7	1.381	1.404	1.429	+0.048
R8	1.441	1.413	1.388	−0.053

[a] See Figure 1 for bond numbering. [b] Difference between the bond length in neutral state and in the dicationic state.

Table 4 summarizes the main skeletal CC bond length distortions for the DPTQtT model compound on going from the neutral form to the radical cation and dication. The UB3LYP/6-31G** optimized geometry of the radical cation as compared with that of the neutral molecule indicates the generation of a positive polaron type defect mainly localized in the inner thiophene rings. The magnitude of the structural modifications progressively decreases from the center of the oligomeric chain toward its ends. The singly oxidized species is characterized by the reversal of the single−double CC bond alternation pattern, especially for the two central units, while the C−S bond lengths were found to be little affected. Thus, the geometry relaxation process upon doping leads to the appearance of a strong quinonoid character within the molecule. As expected, the calculated structural changes are greater in the case of the dication, for which the region with a genuine quinonoid structure extends over the whole oligomeric chain as a consequence of the repulsion between the two positive charges. It can be concluded that the removal of one or two electrons from the neutral oligomer induces geometric changes compatible with the evolution from an aromatic to a quinonoid structure.

A good accordance between the experimental and theoretical spectra is found. The three main Raman bands for the low oxidized species of DHTSxT at 1427, 1397, and 1355 cm^{-1}can be correlated with those at 1422, 1404, and 1382 cm^{-1} in the UB3LYP/6-31** Raman spectrum of the radical cation of DPTQtT. Figure 10 displays the theoretical atomic displacements for the molecular vibrations which give rise to these strong Raman bands. The in-phase ν_s(CC) stretchings of the two inner thiophene rings (i.e., of those units strongly affected by the doping) are mainly involved in the three cases, in combination with different in-phase ν_s(CC) or ν_{as}(CC) stretching motions of the outermost rings of the molecule, so these three collective vibrations are totally symmetric. The Raman intensity of a given band depends on the variation of the molecular polarizability during the specific vibration. In view of the strong enhancement of these three Raman normal modes with respect to the many other totally symmetric vibrations of the molecule, it can be concluded that sizable polarizability changes necessarily must take place during then. These results agree nicely with those previously published by Enhrendorfer et al. for doped oligothiophenes.[16] These authors showed that major changes in the values of the molecular polarizabilities are associated with the ring ν(CC) stretchings of the charged defect generated by the doping.

The B3LYP/6-31G** Raman spectrum of the dication of DPTQtT shows two main bands at 1430 and 1365 cm^{-1} that could be correlated with those experimentally measured at 1391 and 1362 cm^{-1} for the high oxidized species of DHTSxT. The vibrational eigenvectors that give rise to these Raman bands are depicted in Figure 11. As in the radical cation species, these doping vibrations are due to totally symmetric stretchings of those C=C bonds mainly located in the middle of the charged defect. However, in the dication of DPTQtT all the thiophene rings move significantly along each skeletal vibration. Therefore, it could be envisaged that in DHTSxT the bipolaronic defect likely extends over the six thiophene rings, as a result of the electrostatic repulsion between the two positive charges.

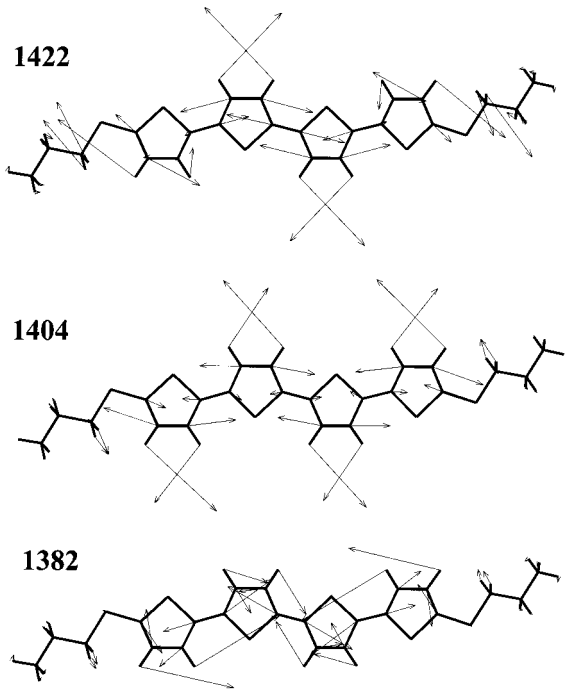

Figure 10. Schematic UB3LYP/6-31G** atomic displacements for the main Raman bands of the radical cation of DPTQtT (all values in cm^{-1}).

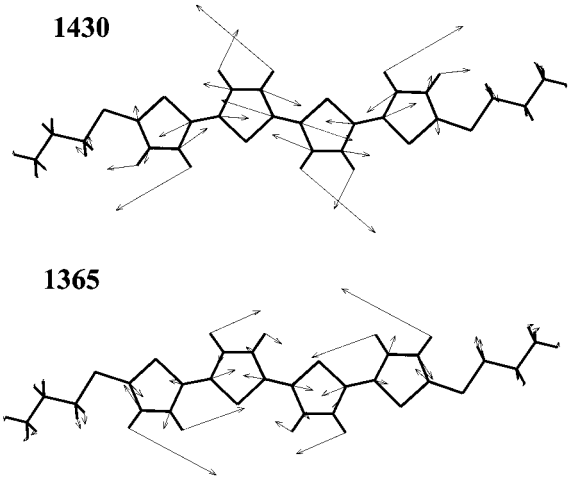

Figure 11. Schematic B3LYP/6-31G** atomic displacements for the main Raman bands of the dication of DPTQtT (all values in cm^{-1}).

The eigenvectors associated with the theoretical Raman bands at 1430 cm^{-1} in the dication, 1422 cm^{-1} in the radical cation, and 1501 cm^{-1} in the neutral species show that the three vibrations are related since they arise from a collective totally symmetric ν_s(C=C) mode, spreading over the whole molecule, in which the motions of the successive thiophene rings take

place in phase. Thus, we can conclude that these Raman bands correspond to the band usually termed line B in the ECC theory.

The ECC theory states that the frequencies of the Raman bands associated with the dynamics of the ECC mode (particularly line B in the case of the oligothiophenes) progressively decrease on increasing doping level. This behavior has been found for DHSxT and DHTSxT; i.e., the strongest band in the experimental Raman spectrum of DHSxT downshifts from 1478 cm^{-1} in the neutral form, to 1442 and 1415 cm^{-1} for the low and high oxidized species, respectively, while for DHTSxT the relevant frequency values are: 1456 cm^{-1} for the neutral form, 1427 cm^{-1} for the low oxidized species, and 1387 cm^{-1} for the high oxidized species. The overall dispersion in DHTSxT is larger than that in DHSxT, particularly, from the radical cation to the dication.

The optimized equilibrium molecular geometries for the neutral, radical cation, and dication species of DPTQtT show that the C_α–S bonds attached to the outermost rings of the chain change by −0.054 Å on going from the neutral to the dication species, while, for example, the inner inter-ring CC bond changes by −0.053 Å. Let us summarize the main changes of the calculated Mulliken atomic charges on going from the neutral molecule up to the dication. The calculations show that atomic charges that support each sulfur atom are mainly affected by the ionization; thus in the dication, each α-sulfur atom supports around 17% of the two positive charges, while each sulfur atom of the thiophene rings supports nearly 12% of the total charge. These theoretical results indicate the strong participation of the α-sulfur atoms in the stabilization of the charged defect, which implies that the spatial extent of the dication in DHTSxT could be larger than that in DHSxT and, at the same time, could justify the observed downshift dispersions of the ECC mode.

VI. Conclusions

The results of a comprehensive study of the vibrational properties of two neutral thiophene-based hexamers bearing two different α,α′-end capped groups (*n*-hexyl vs *n*-thiohexyl) are presented. A full vibrational assignment for the most relevant Raman features of the neutral compounds has been proposed on the basis of RHF/6-31G** ab initio calculations and previous spectroscopic correlations. The resemblance of the Raman spectra of the thiohexyl end-capped sexithiophene and of the unsubstituted hexamer (which were found to be superimposable) suggests that the attachment of sulfur atoms at both end α-positions of the oligothiophene switches off the interactions between the alkyl side chains and the polyconjugated backbone.

The DFT calculations performed for a DPTQtT model compound as radical cation (UB3LYP/6-31G**) and dication (B3LYP/6-31G**) have been used to analyze the evolution of the Raman spectra of DHSxT and DHTSxT upon the electrochemical oxidation of the compounds as thin solid films. The theoretical Raman spectra of the radical cation and dication are found to be rather similar to those of the low and high oxidized species, respectively.

With the help of the theoretical calculations, we have been able to identify the Raman bands associated with the skeletal ν(C═C) vibrations of the radical cation (as a polaron type charged defect) and of the dication (as a bipolaron type charged defect). The molecular geometry calculations and the spectroscopic analysis of the neutral and oxidized compounds demonstrate that the conjugational defect in the radical cation is mainly located in the two or three inner thiophene rings while it spreads over the whole molecule in the case of the dication, due to the repulsion between the two positive charges. The analysis of Mulliken atomic charges and bond lengths reveals that the α-sulfur atoms of DHTSxT have an important participation in the stabilization of the charged defects. This fact could explain the experimental results about the high conductivity of the FET devices made of DHTSxT.

Acknowledgment. The present work was supported in part by the Dirección General de Enseñanza Superior (DGES, MEC, Spain) through the research project BQU2000-1156 and FD97-1765-C03. J.C. is grateful to the Ministerio de Educación y Cultura of Spain for a postdoctoral fellowship at the Department of Chemistry of the University of Minnesota (Plan de Formación y Perfeccionamiento de Doctores y Tecnólogos en el Extranjero, referencia PF00 25327895).

References and Notes

(1) For recent reviews on organics FETs, see: (a) Katz, H. E.; Dodabalapur, A.; Bao, Z. *Handbook of oligo- and polythiophenes*; Fichou, D., Ed.; Wiley-VCH: Weinheim, FRG, 1999; p 459. (b) Katz, H. E.; Bao, Z.; Gilat, S. L. *Acc. Chem. Res.* **2001**, *34*, 359.

(2) (a) Drury, C. J.; Mutsaers, C. M. J.; Hart, C. M.; Matters, M.; de Leeuw, D. M. *Appl. Phys. Lett.* **1998**, *73*, 108. (b) Garnier, F.; Hajlaoui, R.; Yassar, A.; Srivastasa, T. *Science* **1994**, *265*, 1684.

(3) Katz, H. E.; Bao, Z. *J. Phys. Chem. B* **2000**, *104*, 671.

(4) Garnier, F.; Peng, F. Z.; Horowitz, G. *Adv. Mater.* **1990**, *2*, 592.

(5) (a) Katz, H. E.; Lovinger, A. J.; Laquindanum, J. G. *Chem. Mater.* **1998**, *10*, 457. (b) Katz, H. E.; Laquindanum, J. G.; Lovinger, A. J. *Chem. Mater.* **1998**, *10*, 633.

(6) Mitschke, U.; Bäuerle, P. *J. Mater. Chem.* **2000**, *10*, 1471.

(7) Shirota, Y. *J. Mater. Chem.* **2000**, *10*, 1.

(8) Raimundo, J. M.; Blanchard, P.; Brisset, H.; Akoudad, S.; Roncali, J. *Chem. Commun.* **2000**, 939.

(9) Horowitz, G.; Fichou, D.; Peng, X.; Xu, Z.; Garnier, F. *Solid State Commun.* **1982**, *41*, 72.

(10) Garnier, F.; Yassar, A.; Hajlaoui, R.; Horowitz, G.; Deloffre, F.; Servet, B.; Ries, S.; Alnot, P. *J. Am. Chem. Soc.* **1993**, *115*, 8716.

(11) Horovitz, B. *Solid State Commun.* **1982**, *41*, 72.

(12) Horovitz, B. *Phys. Rev. Lett.* **1981**, *47*, 1491.

(13) Ehrenfreund, E.; Vardeny, Z.; Brafman, O.; Horovitz, B. *Phys. Rev. B* **1987**, *36*, 1535.

(14) Zerbi, G.; Gussoni, M.; Castiglioni, C. *Conjugated Polymers*; Bredas, J.-L., Silbey, R., Eds.; Kluwer Academic Publishers: Dordrecht, The Netherlands, 1991; p 435.

(15) (a) Ludwig, T.; Schweitzer, D.; Keller, H. J. *Solid State Commun.* **1995**, *96*, 961. (b) Sakamoto, A.; Furukawa, Y.; Tasumi, M. *J. Phys. Chem.* **1994**, *98*, 4635.

(16) (a) Ehrendorfer, Ch.; Karfen, A. *J. Phys. Chem.* **1994**, *98*, 7492. (b) Ehrendorfer, Ch.; Karfen, A. *J. Phys. Chem.* **1995**, *99*, 5341.

(17) (a) Castiglioni, C.; Lopez Navarrete, J. T.; Gussoni, M.; Zerbi, G. *Solid State Commun.* **1988**, *65*, 625. (b) Zerbi, G.; Castiglioni, C.; Lopez Navarrete, J. T.; Tian, B.; Gussoni, M. *Synth. Met.* **1989**, *28*, D359.

(18) Pulay, P.; Fogarasi, G. *Vibrational Spectra and Structure*; Elsevier: Amsterdam, 1985.

(19) *Density Functional Methods in Chemistry*; Labanowski, J. K., Andzelm, J. W., Eds.; Springer: New York, 1991. Scott, A. P.; Radom, L. *J. Phys. Chem.* **1996**, *100*, 16502.

(20) Stephens, P. J.; Devlin, F. J.; Chabalowski, C. F.; Frisch, M. J. *J. Phys. Chem.* **1994**, *98*, 11623.

(21) Katz, H. E.; Dobadalapur, A.; Torsi, L.; Elder, D. *Chem. Mater.* **1995**, *7*, 2238.

(22) Hotta, S.; Waragai, K. *J. Phys. Chem.* **1993**, *97*, 7427.

(23) Frisch, M. J.; Trucks, G. W.; Schlegel, H. B.; Scuseria, G. E.; Robb, M. A.; Cheeseman, J. R.; Zakrzewski, V. G.; Montgomery, J. A.; Stratman, R. E.; Burant, S.; Dapprich, J. M.; Millam, J. M.; Daniels, A. D.; Kudin, K. N.; Strain, M. C.; Farkas, O.; Tomasi, J.; Barone, V.; Cossi, M.; Cammi, R.; Mennucci, B.; Pomelli, C.; Adamo, C.; Clifford, S.; Ochterski, G.; Petersson, A.; Ayala, P. Y.; Cui, Q.; Morokuma, K.; Malick, D. K.; Rabuck, A. D.; Raghavachari, K.; Foresman, J. B.; Cioslowski, J.; Ortiz, J. V.; Stefanov, B. B.; Liu, G.; Liashenko, A.; Piskorz, I.; Komaromi, I.; Gomperts, R.; Martin, R. L.; Fox, D. J.; Keith, T.; Al-Laham, M. A.; Peng, C. Y.; Manayakkara, A.; Gonzalez, C.; Challacombe, M.; Gill, P. M. W.; Johnson, B. G.; Chen, W.; Wong, M. W.; Andres, J. L.; Head-Gordon, M.; Replogle, E. S.; Pople, J. A. *Gaussian 98*, revision A.7; Gaussian, Inc.: Pittsburgh, PA, 1998.

(24) Francl, M. M.; Pietro, W. J.; Hehre, W. J.; Binkley, J. S.; Gordon, M. S.; Defrees, D. J.; Pople, J. A. *J. Chem. Phys.* **1982**, *77*, 3654.

(25) Scott, A. P.; Radom, L. *J. Phys. Chem*. **1996**, *100*, 16502.
(26) Porzio, W.; Destri, S.; Mascherpa, M.; Brückner, S. *Acta Polym*. **1993**, *44*, 26.
(27) Hotta, S.; Waragai, K. *J. Mater. Chem*. **1991**, *1*, 835.
(28) Schaffer, H. E.; Chance, R. R.; Silbey, R. J.; Knoll, K.; Schrock, R. *J. Chem. Phys*. **1991**, *94*, 4161.
(29) Albrecht, C. A. *J. Chem. Phys*. **1961**, *34*, 1476.
(30) Harada, I.; Furukawa, Y. *Vibrational Spectra and Structure*; During, J. R., Ed.; Elsevier: Amsterdam, 1991; *19*, 369.
(31) Hernandez, V.; Casado, J.; Ramirez, F. J.; Zotti, G.; Hotta, S.; Lopez Navarrete, J. T. *J. Chem. Phys*. **1996**, *104* (23), 9271.
(32) Castiglioni, C.; Del Zoppo, M.; Zerbi, G. *J. Raman Spectrosc*. **1993**, *24*, 485.
(33) Hernandez, V.; Ramirez, F. J.; Otero, T. F.; Lopez Navarrete, J. T. *J. Chem. Phys*. **1994**, *100*, 114.
(34) Hernandez, V.; Castiglioni, C.; Del Zoppo, M.; Zerbi, G. *Phys. Rev. B* **1994**, *50*, 9815.
(35) Agosti, E.; Rivola, M. L.; Hernández, V.; Zerbi, G. *Synth. Met.* **1999**, *100*, 101.
(36) Casado, J.; Hotta, S.; Hernandez, V.; Lopez Navarrete, J. T. *J. Phys. Chem. A* **1999**, *103*, 816.
(37) (a) Casado, J.; Bengoechea, M.; López Navarrete, J. T.; Otero, T. F. *Synth. Met*. **1998**, *95*, 93. (b) Zotti, G.; Schiavon, G.; Berlin, A.; Pagani, G. *Chem. Mater*. **1993**, *5*, 620.
(38) (a) Graf, D. D.; Campbell, J. P.; Mann, K. R.; Miller L. L. *J. Am. Chem. Soc*. **1996**, *118*, 5480. (b) Graf, D. D.; Duan, R. G.; Campbell, J. P.; Miller, L. L.; Mann, K. R. *J. Am. Chem. Soc.* **1997**, *119*, 5888.
(39) (a) Bauerle, P.; Segelbacher, U.; Maier, A.; Mehring, M. *J. Am. Chem. Soc.* **1993**, *115*, 10217. (b) Bauerle, P.; Fisher, T.; Bidlingmeier, B.; Stabel, A.; Rabe, J. *Angew. Chem., Int. Ed. Engl*. **1995**, *34*, 303.